Magnetic-field-dependent morphology of self-organized Fe on stepped Si(111) surfaces

M. Cougo dos Santos, J. Geshev, L. G. Pereira, and J. E. Schmidt

Citation: Journal of Applied Physics **106**, 023904 (2009); doi: 10.1063/1.3172926
View online: http://dx.doi.org/10.1063/1.3172926
View Table of Contents: http://scitation.aip.org/content/aip/journal/jap/106/2?ver=pdfcov
Published by the AIP Publishing

Magnetic-field-dependent morphology of self-organized Fe on stepped Si(111) surfaces

M. Cougo dos Santos,[1] J. Geshev,[2,a)] L. G. Pereira,[2] and J. E. Schmidt[2]
[1]*Departamento de Física, Universidade Federal Rural do Rio de Janeiro (UFRRJ), Seropédica, 23890-000 Rio de Janeiro, Brazil*
[2]*Instituto de Física, Universidade Federal do Rio Grande do Sul (UFRGS), Porto Alegre, 91501-970 Rio Grande do Sul, Brazil*

(Received 2 April 2009; accepted 11 June 2009; published online 17 July 2009)

The present work reports on Fe thin films grown on vicinal Si(111) substrates via rf magnetron sputtering. The dependencies of the growth mode and magnetic properties of the obtained iron nanostructures on both crystallographic surface orientation and on the direction of the very weak stray magnetic field from the magnetron gun were studied. Scanning tunneling microscopy images showed strong dependence of the Fe grains' orientation on the stray field direction in relation to the substrate's steps demonstrating that, under appropriately directed magnetic field, Si surfaces can be used as templates for well-defined self-assembled iron nanostructures. Magneto-optical Kerr effect hysteresis loops showed an easy-axis coercivity almost one order of magnitude smaller for the film deposited with stray field applied along the steps, accompanied with a change in the magnetization reversal mode. Phenomenological models involving coherent rotation and/or domain-wall unpinning were used for the interpretation of these results. © *2009 American Institute of Physics*. [DOI: 10.1063/1.3172926]

I. INTRODUCTION

Stepped surfaces obtained on vicinal substrates have attracted much interest in many areas, such as magnetic thin films, one-dimensional structures, self-organized nanoscale patterns,[1–3] and ultrathin films grown on vicinal Si substrates in view of their potential applications in silicon technologies.[4] The effect of the surface symmetry breaking on the magnetic anisotropy (MA) has been investigated by several groups in various systems. For example, growth-induced MA has been associated with directed surface roughness[5] and/or magnetic field[6] during the deposition. In Fe on W ultrathin films[2,7] the steps favor perpendicular to them magnetic moment alignment. MA with easy axis parallel to the step edges, however, has been observed in Fe films on stepped Ag(100).[8]

Although Fe films grown on Si(111) treated with HF showed clear striped structure,[9] atomic steps are rarely observed in HF-treated Si(111) substrates.[10] Simple chemical etching with 40%NH_4F, however, is able to produce such atomically flat surfaces.[11] The surface preparation of Si(111) alone is an actively pursued research area as well, specially for generation of periodically ordered structures to be used as templates. Due to the effect of dissolved oxygen on the flattening process of Si(111) surfaces, visible etch pits often form around single atomic scale defects, such as dislocations.[12] Formation of hillocks during NH_4F etching of vicinal Si(111) surfaces has been also observed.[13]

The influence of the cap layer on the properties of thin Fe films grown on Si(111) has been recently studied. It has been shown that their MA could depend on the thickness of the cap layer as well as on its growth conditions.[14] Strong dependence of the iron growth mode and MA for Fe/Si(111) on the substrate preparation has also been observed.[15] It has been found recently that magnetic field can influence the hydrothermal growth of polycrystalline Co and Ni wires or magnetite chains aligned along the magnetic field direction.[16] In the present work we study the dependence of the morphology and the magnetic properties of self-organized Fe films deposited on vicinal Si(111) surface on both the crystallographic orientation of the stepped Si surface and on the direction of the field from the magnetron during deposition, H_m.

II. EXPERIMENT

The substrates used were of the *p*-type Si(111) wafers, whose resistivities were in the 2–3 Ω cm range, with a miscut angle of 0.5° toward the $[11\bar{2}]$ azimuth, as estimated by conventional x-ray diffractometry (XRD), performed on a Philips X'Pert MRD machine employing Cu $K\alpha$ radiation. The substrate cleaning procedure used is very similar to the one described in Refs. 10 and 12 and is identical to that used in our previous work.[17]

Iron films of thickness $t=6$ and 12 nm were deposited at room temperature onto the Si substrates by means of rf sputtering in 3.2×10^{-4} Torr Ar atmosphere with base pressure prior deposition better than 10^{-7} Torr and deposition rate less than 0.1 nm/s. The target-to-substrate separation was 6.5 cm and the in-plane magnetic field measured at the substrate surface was $H_m=7$ Oe. Along with the XRD, which indicated (111)-textured Fe, the structural characterization was also performed by *ex situ* atomic force microscopy (AFM) and scanning tunneling microscopy (STM) using a Digital Instruments Nanoscope IIIa. The magnetic properties of the

a)Electronic mail: julian@if.ufrgs.br.

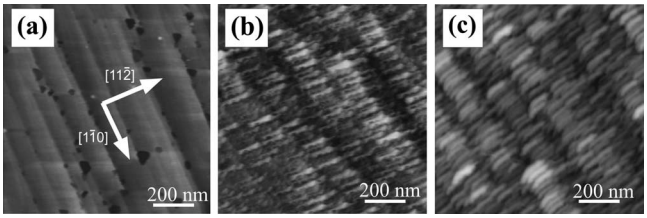

FIG. 1. 1×1 μm^2 AFM and STM images. (a) AFM image of the clean Si(111) substrate. [(b) and (c)] STM images of the 6 and 12 nm thick Fe films, respectively, both grown with H_m parallel to the [11$\bar{2}$] direction.

samples were characterized by *ex situ* magneto-optical Kerr effect (MOKE) magnetometry.

III. RESULTS AND DISCUSSION

The morphology of the substrates and that of the Fe films deposited onto them with H_m aligned along the [11$\bar{2}$] direction are shown in Fig. 1. Panel (a) shows an AFM image of the clean substrate, where large terraces with uniform step height distribution are observed. The mean step height is $\approx$2.1 nm with an average step corner to step edge separation of $\approx$180 nm, a value similar to others reported in the literature.[1] The surface also shows visible hillocks with triangular shape that could be formed by step-step collisions during silicon etching.[13,18] Panels (b) and (c) show the STM topography images of the corresponding Fe(t)/Si(111) films. Extended x-ray absorption fine structure spectra, obtained at room temperature and after MOKE characterization of the films with t=3 nm (Ref. 17) and 6 nm,[19] have shown formation of bcc Fe and no traces of oxide or silicide formation. We recall that for t=3 nm,[17] the iron grows in a form of two distinct types of elongated grains, aligned parallel (with a mean length of $\approx$50 nm) and perpendicular ($\approx$70 nm in length) to the substrate steps, respectively. Apparently, when $H_m\|$[11$\bar{2}$], it turns to be energetically more favorable for the grains that at t=3 nm have long axes parallel to the steps to grow along the perpendicular direction when further increasing t. The iron films studied here are thicker, and parallel-to-the-step grains are no longer visible. At t=6 nm, the grains oriented along the [11$\bar{2}$] direction are bigger (mean length of $\approx$170 nm and width of $\approx$50 nm) than at 3 nm; further increase in t leads to even thicker well-defined elongated grains (for t=12 nm, the grains are $\approx$180 nm long and $\approx$50 nm wide), as seen in panel (c), i.e., the length of the parallel-to-the-step grains at 3 nm is the width for higher thicknesses. Since the length of these nanosized grains corresponds to the terrace width, our results strongly suggest that the steps serve as a matrix for formation of self-assembled iron structure.

We have systematically checked the dependence of the MOKE hysteresis loops and the corresponding coercivity H_C on the in-plane external field angle ϕ_H for the films whose topography is shown in Fig. 1. Figure 2 displays representative loops recorded with the tracing magnetic field H oriented along three crystallographic directions, namely, [11$\bar{2}$], [0$\bar{1}$1], and [1$\bar{1}$0], and Fig. 3 shows the full angle range $H_C(\phi_H)$ variations for the case of H_m parallel to the [11$\bar{2}$] direction. In a previous work[17] we reproduced the data for t=3 nm considering two types of Fe nanosized grains with both cubic and uniaxial anisotropies [in thin films based on a cubic crystal system, such as bcc Fe, sixfold MA in the (111) plane is a natural consequence of the crystalline symmetry and the thin-film geometry; the uniaxial MA comes, in the present case, from the elongated shape of the grains]. The nanograins of each type are all identical and aligned, and every grain of the first type is coupled to the adjacent grain of the other type only.

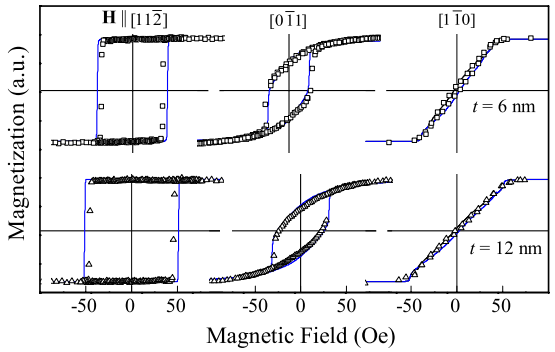

FIG. 2. (Color online) Experimental in-plane hysteresis loops (symbols) for the samples whose surface topology is illustrated in Figs. 1(b) and 1(c); the lines are fittings for tracing field parallel to the [11$\bar{2}$], [0$\bar{1}$1], and [1$\bar{1}$0] directions using $2K_1/M_S$=170 Oe, $2K_2/M_S$=36 Oe, and H_d^{eff}=8.7 kOe, and easy axis along [11$\bar{2}$], where the only parameter varied was $2K_U/M_S$ (=41 and 55 Oe, respectively).

For the higher Fe thicknesses here considered and when H_m is aligned with the [11$\bar{2}$] direction, the magnetization curves show rectangular shape for H along the [11$\bar{2}$] direction (the easy magnetization axis) and loops with very small remanence and coercivity along the perpendicular, i.e., [1$\bar{1}$0], direction (hard axis). These are clear characteristics of dominant uniaxial MA. The $H_C(\phi_H)$ variations, however, show evidences for coexistence of uniaxial and sixfold anisotropies, in accordance with the XRD data. Although the H_C local maxima around the global minima tend to vanish when increasing the Fe thicknesses, they are still visible for t=12 nm.

The above considerations are strongly supported by the numerical calculations (see the solid curves in Figs. 2 and 3). Since there is only one type of nanoparticles for the Fe films

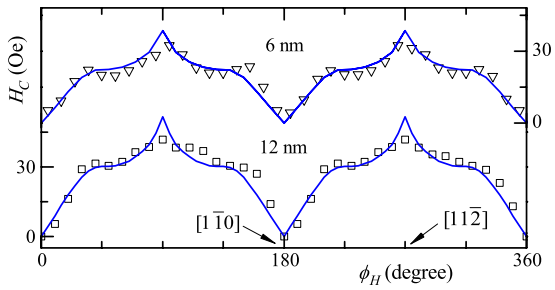

FIG. 3. (Color online) Angular dependencies of the experimentally measured coercivity (symbols) and the corresponding calculated variations (lines) extracted from the hysteresis loop fittings for the Fe films grown with H_m along [11$\bar{2}$]. The parameters used in the calculations are the same as in Fig. 2.

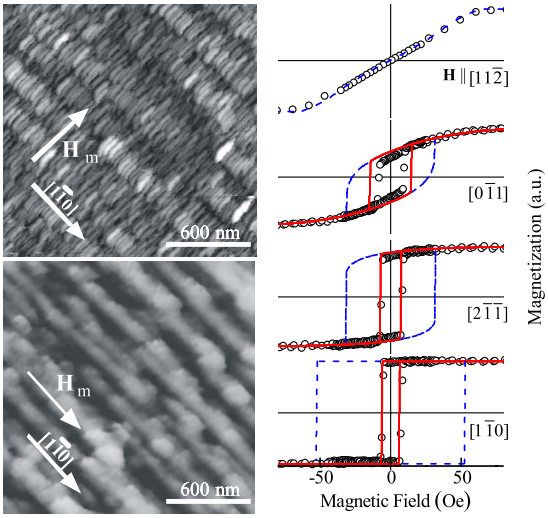

FIG. 4. (Color online) 1.8×1.8 μm^2 STM images of 12 nm thick Fe films grown with magnetron field H_m oriented along the $[11\bar{2}]$ (upper image) and $[1\bar{1}0]$ directions (bottom image), respectively, as well as experimental hysteresis loops (symbols) for the film grown with H_m parallel to $[1\bar{1}0]$. Dashed lines correspond to fittings considering coherent rotation only; solid lines are fittings that involve combined coherent rotation and domain-wall nucleation and sweeping. The parameters used are the same as in Fig. 2 except for $2K_U/M_S=62$ Oe.

here investigated with $t=6$ and 12 nm, the model used to interpret the corresponding experimental data is simpler than that employed to explain the magnetic behavior of the 3 nm thick Fe film.[17] Since it is almost identical to that used in our previous works,[9,15] it will be only sketched here. It takes into consideration a ferromagnet with saturation magnetization M_S, whose total free energy contains cubic and uniaxial anisotropies (being K_1, K_2, and K_U the first two cubic and the uniaxial anisotropy constants, respectively) as well as the effective demagnetization and Zeeman energies. Note that although for magnetization rotation in the (111) plane the cubic anisotropy is given by the K_2 term only, since our Fe films are grown on vicinal Si(111), the magnetization rotation does not necessarily occur in this plane, and the K_1 term must be taken into account as well. Also, the normal-to-the-film direction was chosen to be almost parallel to [111] by taking its polar angle to be 55.2°, thus providing the observed by XRD 0.5° tilt. In all calculations we used $2K_1/M_S=170$ Oe, $2K_2/M_S=36$ Oe, and effective demagnetization field $H_d^{\text{eff}}=8.7$ kOe. Thus, the only parameter actually varied in order to adjust the experimental magnetization was $2K_U/M_S$ since the easy magnetization axis was fixed to be the $[11\bar{2}]$ one. The best fitting for $t=6$ and 12 nm was obtained for $2K_U/M_S=41$ and 55 Oe, respectively.

In order to investigate the effect of the magnetic target field H_m during the film growth, we deposited a 12 nm thick Fe film under the same conditions as above, but with H_m parallel to the steps. As clearly seen in Fig. 4, very different morphology is observed, as compared to the case of H_m perpendicular to the steps [see Fig. 1(c) and the upper image of Fig. 4]. The bottom image in Fig. 4 shows that now the grains grow with their long axes *parallel* to the steps; they are bigger and less defined, i.e., the structure is more stripe-like than particulate. Similar strong influence of the magnetic field, applied during the austenitic decomposition in medium plain carbon steel at slow cooling rate, on the proeutectoid ferrite grain growth has been recently observed by Zhang *et al.*[20] There, it has been attributed to opposing contributions from the atomic dipolar interaction energy of Fe atoms and the interfacial energy, making the elongation along the field direction energetically favorable. In our case, however, the magnetic field with a magnitude of 7 Oe applied during the thin iron films' growth is much lower than that used in the above cited work, i.e., 120 kOe.

The different growth mode for different stray field orientation reflects on the MA and on the switching mechanism as well. It is demonstrated in Fig. 4, where four representative hysteresis loops are plotted. Now, contrary to the sample grown with H_m perpendicular to the steps, $[1\bar{1}0]$ and $[11\bar{2}]$ are the easy and hard axes, respectively. The dashed lines are fittings obtained using the same model (that involves coherent magnetization rotation only) and parameters as above except the slightly higher $2K_U/M_S$ (=62 Oe).

The solid lines in Fig. 4 correspond to calculations that involve combined coherent magnetization rotation and domain-wall nucleation and unpinning,[21] i.e., the rotation is coherent at all fields and angles except near the switching fields. Any irreversible jump is anticipated by spin transition to the nearest lower energy minimum direction, and the switching is mediated by formation and sweeping of a domain wall. Clearly, the irreversible jumps occur at switching fields rather lower than those expected for the coherent rotation mode, being the easy-axis H_C approximately eight times smaller than that for the film with the same thickness but deposited with H_m perpendicular to the steps. Also, the angular variation in the coercivity is in accordance with the Kondorsky relation,[22] i.e., $H_C \propto (\cos\phi_H)^{-1}$, valid for magnetization reversals that take place by nucleation and growth of reverse domains. The very good agreement between the solid curves and the experimental data strongly supports the assumption of such a switching mechanism. The detailed description of the model used to explain the magnetic behavior of this (111)-oriented sample goes beyond the scope of the present letter and will be presented in a forthcoming paper.

In summary, strong dependence of the morphology of self-organized Fe grown onto stepped Si(111) surfaces on the direction of the field from the magnetron during deposition was observed. Magnetization hysteresis loops showed an easy-axis coercivity almost one order of magnitude smaller for the 12 nm thick Fe film deposited with the stray field parallel to the Si steps as compared to the perpendicular configuration, accompanied with a change in the magnetization reversal mode. Phenomenological models involving coherent rotation and/or domain-wall unpinning were used for the interpretation of these results. We demonstrated that, under appropriately directed magnetic field, stepped Si surfaces can be used as templates for well-defined self-assembled iron nanostructures. Their size, orientation, and magnetic properties can be tuned by varying the substrate cut, its orientation during deposition, and the film thickness.

ACKNOWLEDGMENTS

This work was supported by the Brazilian agencies CNPq and CAPES.

[1]J.-L. Lin, D. Y. Petrovykh, J. Viernow, F. K. Men, D. J. Seo, and F. J. Himpsel, J. Appl. Phys. **84**, 255 (1998).
[2]H. J. Elmers, J. Hauschild, and U. Gradmann, J. Magn. Magn. Mater. **221**, 219 (2000).
[3]F. K. Men, F. Liu, P. J. Wang, C. H. Chen, D. L. Cheng, J. L. Lin, and F. J. Himpsel, Phys. Rev. Lett. **88**, 096105 (2002).
[4]M. Eddrief, Y. Wang, V. H. Etgens, D. H. Mosca, J.-L. Maurice, J. M. George, A. Fert, and C. Bourgognon, Phys. Rev. B **63**, 094428 (2001).
[5]Y. Park, E. E. Fullerton, and S. D. Bader, Appl. Phys. Lett. **66**, 2140 (1995).
[6]E. Simpson, E. Persson, W. Bonin, and E. Wuori, IEEE Trans. Magn. **20**, 782 (1984).
[7]J. Chen and J. L. Erskine, Phys. Rev. Lett. **68**, 1212 (1992).
[8]R. K. Kawakami, E. J. Escocia-Aparicio, and Z. Q. Qiu, Phys. Rev. Lett. **77**, 2570 (1996).
[9]M. Cougo dos Santos, J. Geshev, J. E. Schmidt, S. R. Teixeira, and L. G. Pereira, Phys. Rev. B **61**, 1311 (2000).
[10]K. Itaya, R. Sugawara, Y. Morita, and H. Tokumoto, Appl. Phys. Lett. **60**, 2534 (1992).
[11]M. H. Wang and L. J. Chen, Appl. Phys. Lett. **62**, 1603 (1993).
[12]C. P. Wade and C. E. D. Chidsey, Appl. Phys. Lett. **71**, 1679 (1997).
[13]J. Flidr, Y.-C. Huang, T. A. Newton, and M. A. Hines, Chem. Phys. Lett. **302**, 85 (1999).
[14]R. Stephan, A. Mehdaoui, D. Berling, D. Bolmont, G. Gewinner, P. Wetzel, S. Zabrocki, S. Hajjar, G. Garreau, J. L. Bubendorff, and C. Pirri, J. Magn. Magn. Mater. **293**, 746 (2005); R. Stephan, A. Mehdaoui, D. Berling, and P. Wetzel, J. Appl. Phys. **105**, 013919 (2009).
[15]M. Cougo dos Santos, J. Geshev, D. K. Silva, J. E. Schmidt, L. G. Pereira, R. Hubler, and P. Allongue, J. Appl. Phys. **94**, 1490 (2003).
[16]H. Niu, Q. Chen, H. Zhu, Y. Lin, and X. Zhang, J. Mater. Chem. **13**, 1803 (2003); H. Niu, Q. Chen, M. Ning, Y. Jia, and X. Wang, J. Phys. Chem. B **108**, 3996 (2004); M. Wu, Y. Xiong, Y. Jia, H. Niu, H. Qi, J. Ye, and Q. Chen, Chem. Phys. Lett. **401**, 374 (2005).
[17]M. Cougo dos Santos, J. Geshev, L. G. Pereira, M. C. M. Alves, J. E. Schmidt, and P. Allongue, Phys. Rev. B **70**, 104420 (2004).
[18]J. Flidr, Y.-C. Huang, and M. A. Hines, J. Chem. Phys. **111**, 6970 (1999).
[19]M. Cougo dos Santos, Ph.D. thesis, Universidade Federal do Rio Grande do Sul, 2004.
[20]Y. D. Zhang, C. Esling, J. Muller, C. S. He, X. Zhao, and L. Zuo, Appl. Phys. Lett. **878**, 212504 (2005).
[21]R. P. Cowburn, S. J. Gray, J. Ferré, J. A. C. Bland, and J. Miltat, J. Appl. Phys. **78**, 7210 (1995); R. P. Cowburn, S. J. Gray, and J. A. C. Bland, Phys. Rev. Lett. **79**, 4018 (1997).
[22]E. Kondorsky, J. Phys. (USSR) **2**, 161 (1940).